Nuclear Instruments and Methods in Physics Research B 122 (1997) 427–441

ELSEVIER

NIM B
Beam Interactions with Materials & Atoms

Molecular-dynamics simulation of sputtering

Herbert M. Urbassek

Fachbereich Physik, Universität Kaiserslautern, Erwin-Schrödinger-Straße, D-67663 Kaiserslautern, Germany

Abstract

A review is given on the method of molecular-dynamics computer simulation, and on the results obtained on the physics of sputtering. On the methodological side, the physical input (such as the interatomic potentials, coupling to the electronic system), the reliability, and computer time requirements of simulations are discussed. Molecular-dynamics results obtained after 1992, the time of the last review, are presented. Those results are emphasized, which are difficult to be obtained by other theoretical or computational means: sputtering from high-energy-density zones (spikes), cluster emission, formation of surface topography and their influence on sputtering, and chemical effects.

1. Introduction

Sputtering is defined [1–4] as the emission of (neutral or charged) atoms due to the bombardment of a surface by a single projectile; usually the projectile is an ion, but as well atoms and clusters may be employed. Note that this definition excludes more general erosion phenomena such as beam induced evaporation, which cannot be attributed to a single ion. However, in the case of laser irradiation, sometimes the term *laser sputtering* is used [5], even though the quantum yield (desorbed atoms/photon) may be a highly non-linear function of the laser intensity (number of photons). In this review, I will concentrate on atom or cluster induced sputtering.

The theoretical understanding of the sputter phenomenon is quite mature. While molecular-dynamics computer simulations were performed very early in the field of atom solid interaction [6], the main progress in understanding of the sputter phenomenon came through analytical theory [7]. It identified the physical mechanism by which sputtering proceeds in the majority of cases: the linear collision cascade, in which the energy and the momentum of the impinging projectile ion is distributed among (primary knock-on) target atoms, and from these further on to secondary recoils, until a near-surface target atom, which has received a sufficiently high outward-directed momentum, is sputtered from the surface. Soon then computer simulation schemes were established, to give a more detailed atomistic picture of the collision cascade. They were based on the binary-collision approximation (BCA), by which every moving atom only collides with one target atom at a time. With the further assumption that moving atoms only collide with target atoms at rest, such codes efficiently implement the idea of a linear collision cascade on the atomic level. While target crystallinity can well be included – here MARLOWE is a prominent example [8] – a further speed-up can be obtained, when the target is considered as structureless (amorphous or polycrystalline); such codes have been named Monte Carlo (MC) codes, and here TRIM is a well-known example [9]. A recent review of computer simulation in ion–solid interaction is given in Ref. [10].

These BCA and MC codes thus have a fairly well defined physical picture behind them; since they are quite fast, they have been frequently employed, and often give a very good representation of experimental results. However, there are two drawbacks. First, these codes need a number of simulation parameters – such as the surface- or bulk-binding energy – the values of which are sometimes unclear and have to be fitted to experimental data; this may present in fact a considerable problem in particular in the case of compound sputtering. This situation is unsatisfactory from a fundamental point of view, as long as these parameters are not understood from the attractive part of the interatomic potential. Second, there are sputter phenomena outside the linear-cascade regime: sputtering may occur from zones of high-energy density (spikes), where moving atoms interact with other moving atoms, and the concept of the *linear* cascade breaks down. Another example is the sputtering of (large) clusters, where the effect of interatomic attractive forces is crucial for describing cluster formation and survival. Also chemical effects in sputtering, such as in ion-beam etching or in compound sputtering, can be modelled in BCA or MC codes only via the introduction of ad hoc parameters. Fig. 1 gives an example of the application of the molecular-dynamics method to sputtering, showing on an atomistic scale the dramatic processes which occur in an ion-bombarded target at the surface, and the resulting sputtering (cf. Section 3.2).

The technique of molecular-dynamics simulation is able

PII S0168-583X(96)00681-7

to deal with all kinds of sputter phenomena, as long as the interatomic interaction forces are realistically modeled. Introduced in the 60s, molecular-dynamics simulations have become more and more widespread recently due to the progress in available computer power. From the knowledge of the interatomic forces, the motion of the projectile and of a sufficiently large number of target atoms can be calculated. The spike regime is not any more difficult to simulate than the linear sputter regime. Cluster emission, or any other effect which depends on the details of the interatomic attraction, is easily calculated, as soon as a potential is available which describes the attraction in the solid, at the surface, and in the cluster equally well. With the advent of potentials that incorporate chemical bonding effects, chemical effects in sputtering could be simulated.

The availability of realistic interatomic potentials and of sufficient computer power are the main factors which restrict the applicability of molecular dynamics. In detail, however, a number of other considerations enter which limit the trustworthiness and reliability of molecular-dynamics simulations. Their enumeration and discussion will constitute the main contents of Section 2. A number of results on the subject of sputtering will be presented in Section 3, where attention is focused on those issues where no other theoretical technique can easily compete with this method: spikes, cluster emission, surface topography and chemistry.

This review hence aims at expressing all the *caveats* which need to be considered in order to perform reliable calculations, and to delineate those areas of research, where molecular-dynamics simulation can be considered to be leading the theoretical progress, or at least has contributed its part to the understanding of sputter phenomena. Since the last reviews on the field of computer simulation including molecular dynamics in sputtering are found in Refs. [10–14], and cover work up to around 1992, here results obtained after this time will be discussed.

2. Method

Molecular-dynamics simulation in the present context is a technique using *classical* mechanics to calculate the time evolution of a system of particles. While in other applications of molecular-dynamics techniques – such as for describing the equilibrium properties of solids and clusters – quantum methods are increasingly being used [15], the simulation of particle–solid interaction using a quantum-mechanical framework has been extremely rare; I mention the simulation of carbon penetration into a carbon film [16], and of the growth of a silicon film using hyperthermal silicon atoms [17]. Solving the classical equations of motion requires physical input: the forces on the particles need to be specified. This is done by providing expressly the interatomic potentials, which will for most materials of interest be of a many-body nature. However, moving atoms may couple to the electrons, resulting in energy loss and electronic excitation. But also the boundary conditions applied on the system of target particles represent physical input, viz. the reaction of the surrounding material on the simulated volume. Finally, the initial state of the projectile and the target need to be specified.

Technically the integration routine which is used to solve the equations of motion and in particular the time step which they necessitate are important. Also, the question when a simulation is ended needs to be addressed. The issue of how to detect a sputtered particle may sound trivial, but complexities appear at least in the case of cluster emission. Finally, sputtering is a stochastic process, in the sense that the sputter yield of a particular ion depends on its precise point of impact. We shall discuss all these issues in their order of enumeration below.

There exist quite a many books on the technique of molecular-dynamics simulation [10,18–25], most of which address general problems of materials in thermodynamic equilibrium. The question of ion–solid interaction is usually not addressed very broadly in these monographs, if at all [18,26], with the exception of Ref. [10], which however concentrates on MC and BCA methods. Since there are some aspects which are very specific to this application – e.g., a strongly non-equilibrium situation is treated, the interatomic potential is needed from very close distances corresponding to keV relative energy through the equilibrium bonding distance to large separations –, it is worthwhile to discuss here in detail some of the specific problems which enter the field of molecular-dynamics simulations of sputtering.

2.1. Potentials

The definition of the interatomic potential constitutes the essential physical input to a molecular-dynamics simulation. Ideally, it is the *only* physics input – at least, as long as electronic excitations are not important. Whereas before around 1985 only pair potentials were used, nowadays a considerable variety of potential forms have been established, which describe different classes of materials [27]. For a discussion of the potential functions, a distinction between high-energy potentials – valid above roughly 100 eV, although the exact limit varies from system to system – and low-energy potentials – which are derived to describe the bonding region below 0 eV – is in order.

(1) The high-energy potentials employed in molecular dynamics describe the close interaction of 2 atoms, where in most situations the influence of the environment can be neglected. Hence, the high-energy potential is appropriately derived from a quantum-mechanical calculation of the total energy of a dimer in vacuum. Either quantum-chemical methods are applied for the atom pair of interest [14], or one of the many scaling potential forms commonly in use – such as the Molière- [28], Kr–C- [29], or ZBL-potential [30] – is employed. The high-energy potential is in principle just the same as that used in BCA or MC calculations [10].

(2) The low-energy potential describes the bonding of the atom in its equilibrium situation in the solid, and at small deformations around the equilibrium [31]. Ideally, the potential used is flexible enough to describe as well the bonding in the solid, at the surface, around defects, in dimers and clusters. Since the bonding in these situations depends in many materials on the environment, the low-energy potential usually contains a many-body contribution in addition to a (repulsive) pair-interaction term. For metals, the potentials of the embedded atom method (EAM) [32–34] or of a tight-binding form [35–37] are most commonly used. These potentials are of empirical or semi-empirical origin. However, there are a number of attempts to give these potentials a more ab initio grounding [38,39]. For covalent materials, another class of potentials using explicitly the dependence on the bond angle, has been created, of which the so-called Stillinger–Weber potential [40] is a prominent example. A more generic form seems to be available through the so-called bond-order potentials [41,42]. Clearly, van der Waals bonded materials can be described to a good degree by pure pair potentials, although even there many-body contributions need to be included to get accurate agreement between experiment and theory of equilibrium systems, such as in condensed noble gases [43]. Finally, in ionically bonded systems, a Coulomb contribution must be included. In principle, this is definitely possible, and has been done, e.g. in the simulation of SiO_2 [44,45], but not yet for sputtering studies. However, extra computational problems arise, since the Coulomb potential decays so slowly that it cannot be cut off and techniques such as Ewald summation [20] must be used; potentials in non-ionic systems, on the other hand, are usually cut off at a distance r_c (cut-off radius) and as a consequence, the number of interaction partners of any atom is small.

A great deal of physics important for sputtering occurs at 0 to 20 eV interaction energy, since this is precisely the range of energies where most particles are sputtered. Unfortunately in this energy range, not much independent experimental or theoretical knowledge on the potential is available. From a practical point of view, this gap is closed by splining together the high- and low-energy potentials. This is usually done for a dimer in vacuum, and leaves some arbitrariness in assigning the potential in particular for its many-body contribution. Other authors simply spline the high-energy potential to the repulsive part of the many-body potential. More work has to be performed to get a deeper understanding on the potential in this important regime, both on the experimental and the theoretical side [46]. In particular, information on the defect creation should allow one to assess the potential, since the displacement threshold is in many materials situated in the middle of the energy regime in question, at 20 to 40 eV [47,48].

2.2. Electrons

In a classical molecular-dynamics simulation scheme, electrons are by necessity not included as dynamic objects. They only appear as sources for energy loss or gain in the equations of motions of the atoms, or by the introduction of (adiabatic) excited-atom interaction potentials. Hence, as soon as electrons play an important role in the ion–solid interaction or sputtering process, the physical input to molecular dynamics stands on a less well defined basis. In the case of metals, electronic excitations are primarily regarded as a way of energy loss from the ion or target atoms; this energy loss is included in the same way – i.e., as a friction-like force [49], or (for inner-shell excitation) as a localized energy loss upon collision [50] – as in BCA or MC calculations [10]. Various formalisms of how to include the coupling to electrons have been set up [14,51–55] by making use of the idea that at small atom energies the interaction must be given by the electron–phonon coupling as employed in standard metallic conduction theory. Examples will be discussed in Section 3.2.

In the case of insulating targets, electronic excitations are long-lived, and can lead to *electronic* sputtering [56], when the potential energy stored in the electronic excitation is relieved to kick an atom off the surface. Such electronic sputtering processes have been modelled ad hoc employing molecular dynamics, by switching the interatomic potential from an excited potential surface to the ground-state potential surface [57].

2.3. Boundary conditions and system size

Ideally, such a large target system should be simulated that no information of the impinging ion reaches the target boundary before all sputtering has ended. Practically, this can never be performed. Instead, a small target system is simulated, and the reaction of the surrounding environment is modelled via the introduction of suitable boundary conditions. The obvious way how to study the appropriateness of boundary conditions is to perform the same simulation for varying boundary conditions and system sizes, and to analyze the action of the boundary conditions. Such a systematic study does not seem to have been performed in the literature, even though partial results have been published [58].

In actual terms, the target system to be studied is often chosen to be rather small for sputtering studies. As an example, for the case of 5 keV Ar on Ag(111) bombardment, Wucher and Garrison used of the order of 2300 target atoms [59], and Betz and Husinsky around 6200 for the comparable Cu(111) target [60]. Even for the largest system size quoted, usually the cascade is not enclosed in the target volume, i.e., target atoms are ejected also on the lateral and bottom sides of the simulation volume. The credibility of this approach lies in the fact that the linear-cascade sputter yield is proportional to the energy deposited in the near-surface layers of the target. As long as the lateral size

of the target is sufficiently large to contain the cascade, and the target is sufficiently deep to correctly simulate all projectile or energetic target atom reflection back towards the surface, the sputter yield will be reasonably described. It would be helpful, however, if some sort of systematic information on the number of target atoms necessary to perform a reliable sputter simulation and on the dependence of the necessary size of the simulation volume on the bombarding energy were available. This does not appear to be the case.

The boundary conditions employed may be divided into four groups:

(i) *Free boundaries*, where actually the bombardment of a large cluster in vacuum is studied;
(ii) *Fixed boundaries*, where except at the free surface, boundary atoms are nailed to their positions, or equivalently may vibrate in oscillator potentials, but can not be displaced;
(iii) *Damping boundaries*, where except for the free surface, a friction-like force acts on all boundary atoms.
(iv) *Laterally periodic* boundary conditions.

Combinations of these groups are possible. Fixed boundary conditions suffer from the fact that energy and momentum will be reflected from the boundaries back into the simulation volume. To a lesser extent, this also happens at free boundaries. Damping boundary conditions are assumed to give a better description of the reaction of the surrounding material on the energy and momentum input to it from the simulation volume. In other words, the heat conduction and pressure relaxation of the surrounding solid shall be modelled. One prescription is to choose the damping constant such as to simulate the critical damping of a harmonic oscillator vibrating at the Debye frequency of the material [18]; another one derives the damping from the target heat conductivity [61]. Laterally periodic boundary conditions give a consistent representation of the reaction of the surrounding material at the cost of artificially simulating an infinite number of closely-spaced simultaneous ion impacts. These boundary conditions have been applied in particular for growth studies [17,62]. In investigations, where the target response is critical, even more refined procedures are employed, such as Langevin dynamics in the boundary layer [63,64].

A systematic study of the effect of the boundary conditions on sputter simulations for a specific system, such as Ar bombardment of a Cu target, would be clearly a help in designing future sputter simulations, but appears not to be available. We note, however, the related investigation in Ref. [65] of the influence of dissipative boundary conditions for a radiation damage simulation.

It should be mentioned that as a rule, the system size necessary for sputter studies will be smaller than for other ion–solid interaction studies, such as formation and relaxation of bulk defects and surface topography, etc., since these occur usually on a longer time scale than sputtering, and the material reaction must be modelled with care. An exception may be given by spike emission phenomena, since there sputtering may last for a longer time, and be more closely related with the fate of the surrounding material.

2.4. Initial state

Often calculations are performed on a crystalline target at zero temperature. This defines the target structure perfectly well, unless that the relaxation or reconstruction of the target surface needs to be taken into account. Note that while an unrelaxed surface is not in equilibrium and will relax even if no kinetic energy is initially available, an unreconstructed surface will stay in its metastable equilibrium for an indefinite time at zero temperature. The effect of surface reconstruction on the sputter yield may be quite dramatic; thus an almost 40% decrease of the sputter yield of 1 keV Ar on (100) Si has been found on reconstruction, due to the higher surface-binding energy of the reconstructed surface [66]. In comparison, the effect of relaxation on the sputter yield is relatively small. An increase of the sputter yield of 6% upon relaxation has been found for 1 keV Ar bombardment on Pt(111) [67].

A different situation arises if a target with an irregular surface is bombarded. Such a case arises for amorphous targets, targets with a random surface topography, for random alloys, or for targets at a pre-defined non-zero temperature. In these cases it will be important that every new projectile which impinges on the target hits a fresh surface, uncorrelated from the surface of the previous ion. This will usually mean that in the case of an alloy, for each new projectile, a new alloy target is created; etc. In the case of amorphous targets, it is usually too time-consuming to create new amorphous targets each time a new projectile impacts; here often only different areas of the same amorphous specimen are bombarded.

2.5. Integrator

Quite a large number of integrators of ordinary differential equations have been employed in molecular-dynamics simulations. They vary in their numerical order, which defines on the one hand the order of the derivatives of the potential which is needed; on the other hand, a higher order implies that a larger time step could be chosen for a comparable accuracy. This reasoning holds true for smooth integrands, but will not apply so stringently to cut-off potentials. Furthermore, while a higher order may give a higher accuracy of the calculation, it needs more memory. Hence, many simulators use the simple second-order (velocity-form) Verlet algorithm [20]. Other, more refined integrators are of a predictor-corrector form such as the Gear algorithm [68]. Note that in contrast to the velocity-form of the Verlet algorithm, other integrators are often not time-reversion symmetric; this applies in particular to those of the predictor-corrector class. This may be a disadvantage if trajectory reversion is used to test the accuracy of the calculation. Several advantages or disadvantages of these integrators have been

discussed in the literature [18,20,69,70]. Note that some integrators cannot handle dissipative forces, and hence cannot be used with electron–phonon coupling or dissipative boundary conditions.

A particular problem, which is encountered in every simulation, is the choice of the time step. Usually, the time step is increased in the course of a sputter simulation when particles slow down. The size of the time step is to be determined from the relative accuracy with which results are needed; this is usually performed in a pragmatic way by halving or doubling its value and repeating the calculation. For the Verlet algorithm, a useful criterion is that the time step should be so small that it allows the fastest particles to travel not farther than 5% of the nearest-neighbor distance [18]. Sometimes it is required in addition that the forces do not change too strongly during one time step.

2.6. Termination

Obviously the simulation should be ended, after the last sputtered particle has left the target. However, this is not easy to recognize. Thus, in practice an energy criterion has been used, which terminates the simulation when the kinetic energy of every atom has dropped below the cohesive energy of the system, or of a certain fraction of it. While this criterion may work fine in the linear-cascade regime, it must be more thoroughly tested in a spike scenario. In other work, the simulation is simply ended after a fixed time has elapsed after the ion impact, 1 ps for example. Again, the justification is not simple and may mean in practice that a number of late sputtered atoms are missed.

2.7. Detectors

Their prime task is to detect a sputtered atom at the end of the simulation. It is defined as an atom with no other atom in the cut-off radius of the potential, i.e., with zero potential energy. If the sputtered atom is part of a cluster, this definition is applied to the cluster as a whole. A convenient way to detect sputtered clusters is to perform a recursive search through the nearest-neighbor list to be defined in Section 2.9 [71]. In the case that the sputter simulation is performed with a small target system, which does not contain the entire collision cascade, atoms and clusters will be emitted on all sides of the crystal. Then care must be taken to discriminate against atoms emitted from the sides of the target volume in an oblique direction towards the surface.

In some work, sputtered particles have been defined by a distance criterion with respect to the original surface plane. In this case, care must be taken that the surface topography developing as a consequence of the ion impact will not disturb the analysis, cf. Fig. 1.

Emitted clusters have been found to be metastable both in experiment and simulation [72] and to fragment on the time scale of several up to at least several hundred ps. The analysis of these time-dependent cluster distributions will be discussed in Section 3.3 below.

2.8. Statistics

Sputtering constitutes a stochastic process, in that the sputter yield strongly fluctuates from one to the other single ion impact. We note that for large cluster impact, fluctuations are considerably reduced.

For a single crystal with a perfect surface at temperature zero, the surface crystallographic structure defines an irreducible surface element; using the symmetry and translation invariance of the surface, ion bombardment into this irreducible surface element is representative of ion bombardment of the entire surface. Actually, denoting the lateral coordinates in the irreducible surface element by $\boldsymbol{\rho}$, the sputter yield of an ion which impinges normally onto the surface and aims at $\boldsymbol{\rho}$ can be designed as $y(\boldsymbol{\rho})$. From this point of view, molecular dynamics can be seen as a means of calculating the function $y(\boldsymbol{\rho})$. For comparison with experiment, what is actually needed, is the mean value $Y = \int \mathrm{d}^2\rho\, y(\boldsymbol{\rho})/A$, where A is the area of the irreducible surface element. Such an integral can be performed by Monte Carlo integration: by shooting at random a number of N_{ion} ions onto the surface, the average Y can be calculated with a relative error proportional to $1/\sqrt{N_{\mathrm{ion}}}$. Note, however, that the constant of proportionality may be large, since the standard deviation of the sputter yield is of the size as the average yield itself [73].

This is the approach usually taken; often, however, a subdivision of the irreducible surface element into smaller cells is performed, and a MC integration is performed in each of the cells [12]. This technique is called "stratified Monte Carlo"; when properly implemented – this requires in particular a clever positioning of the boundaries of the small cells, and hence some prior knowledge of $y(\boldsymbol{\rho})$ – it will accelerate the convergence of the entire calculation [74]. Another method uses the so-called quasi-random or low-discrepancy numbers, which improve the convergence behavior to $1/N_{\mathrm{ion}}$ [74–76]. Alternatively, one might prefer to evaluate $y(\boldsymbol{\rho})$ on a regular grid in the irreducible surface element. Such a procedure would be more reminiscent of the handling of the averaging problem by one of the many numerical quadrature rules available, such as Simpson's rule [77]. However, such a rule does not seem to have been applied yet, obviously because it requires some smoothness properties of $y(\boldsymbol{\rho})$. Actually, $y(\boldsymbol{\rho})$ is a discontinuous and rather irregular function, due to the chaotic trajectories which atoms perform in the collision cascade [78]. Fig. 2 gives a view of the irregularity of $y(\boldsymbol{\rho})$ for a particular case.

If the target system is at a non-zero temperature, the ensemble average of Y with respect to target temperature must be calculated. It is not known how much this averaging complicates the calculation, since while more randomness is included because of target disorder, the function $y(\boldsymbol{\rho})$ may actually look smoother when temperature averaged.

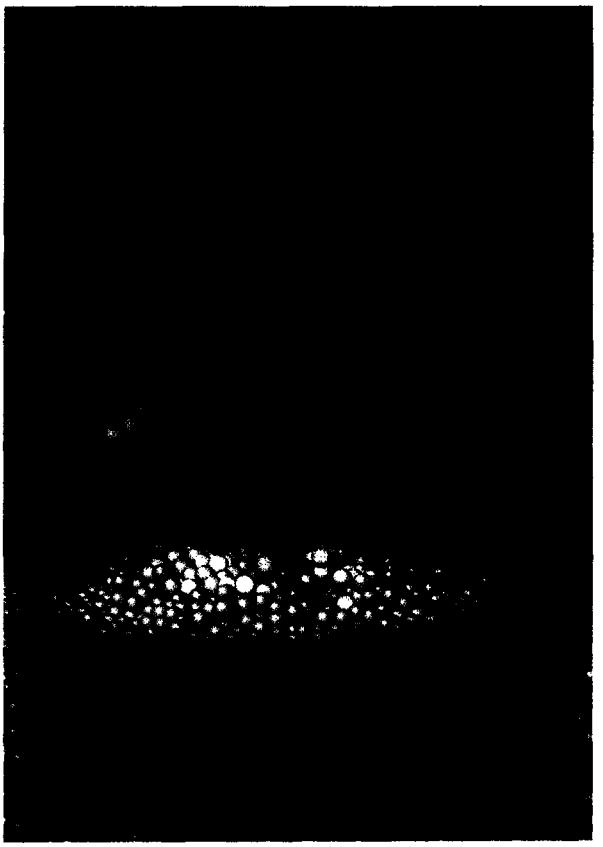

1A

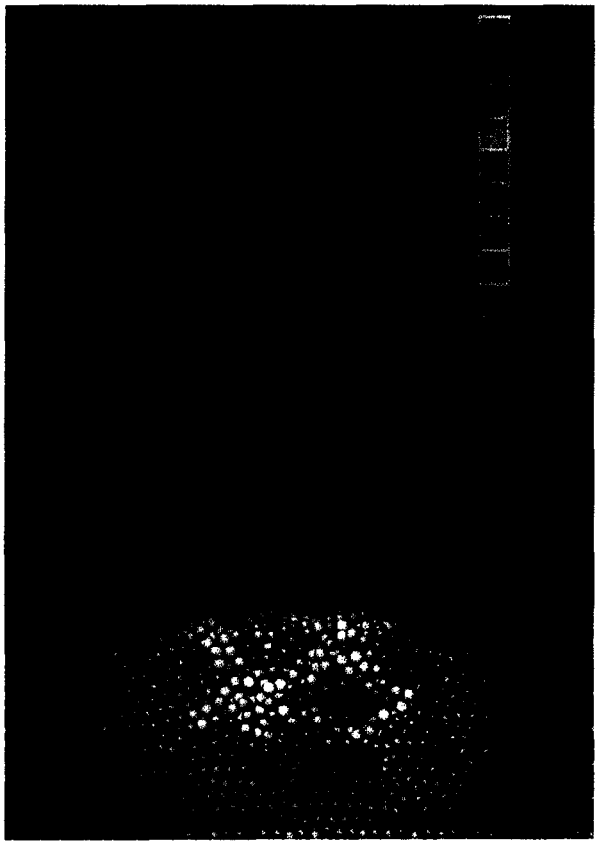

1B

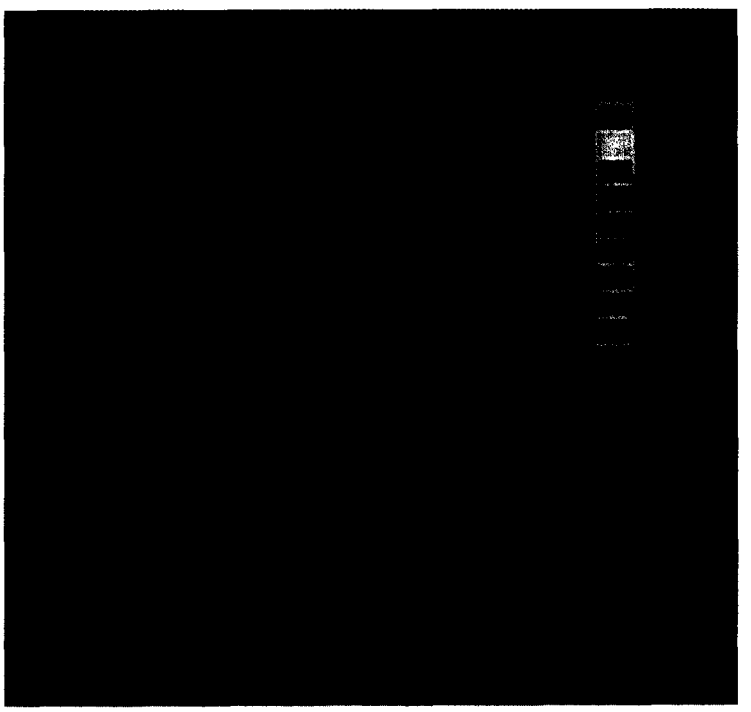

2

Fig. 1. (previous page) Cu (111) crystal 1 ps after bombardment with a 5 keV Cu atom. (a) View of the surface and sputtered particles. (b) Cross section cutting through the point of ion impact. Color code: "Temperature" in units of the melting temperature. See text, Section 3.2.

Fig. 2. (previous page) Sputter yield $y(p)$ shown as a function of the lateral impact parameter p of the bombarding ion. p is varied in the irreducible surface element of the fcc (111) surface: a surface atom is at the position of the left triangle vertex, a 2nd layer atom at the right, and a 3rd layer atom at the top. Data is taken for 4000 impacts of 600 eV Ne ions on a relaxed Pt (111) surface. The mean yield is $Y = 1.6$.

2.9. Computer time requirements

Neglecting code initialization, the CPU time t_{cpu} is proportional to the number m of time steps performed. Furthermore, for sufficiently large numbers of atoms N, the CPU time is proportional to N, $t_{cpu} = \alpha N m$. α then is the CPU time per time step and per atom. It is best measured in FLOP (floating point operations). To this end, the measured CPU time is divided by the speed of the computer used. The speed of the RISC/6000 workstation we used is 23 MFLOPs, where 1 FLOPs denotes 1 FLOP per second.

The N-proportionality of t_{cpu} is due to the fact that we have a finite cut-off radius, i.e., the number of atoms N_c with which any particle interacts is finite. Since the identity of the interaction partners changes with time as a consequence of particle motion, neighbor lists are used; these are bookkeeping devices to identify the interaction partners, and need to be continuously updated. Fig. 3 shows that in particular for large particle numbers, it pays well off to use an intelligent neighbor list. The best list nowadays in use is the Verlet–linked-cells algorithm [79]. In the linked-cells algorithm the simulation volume is divided up into a regular lattice of cubic cells; each particle is assigned to the cell in which it momentarily lives; this routine is very fast. If the edge length of the cell is chosen identical to the cut-off radius of the potential, all interaction partners of a particular atom are found in the very same or in any of the 26 neighboring cells. Verlet lists [80] use spheres around each atom; by choosing the radius of the spheres equal to the cut-off radius, all the atoms within the Verlet sphere of a particular particle are by definition its interaction partners. Using a second, larger sphere concentric with the first one (the so-called Verlet skin), the Verlet list needs not to be updated at every time step. As Fig. 3 shows, the combination of spherical and cubic cells works most efficiently. Note that the pure Verlet scheme exhibits an N^2 scaling of the cost at each update.

Fig. 3 also shows that a typical many-body potential as used for a metal is somewhat more than double as slow as a typical pair potential. Depending on the cost of analytical function evaluation, potentials are encoded as look-up tables rather than as analytical expressions to be evaluated. As a consequence of the structure of metallic many-body potentials, three tables instead of one need to be looked up for the force calculation: one for the pair potential part, and two for the many-body part. Since the force calculation is the most time-consuming part of the molecular-dynamics program, a factor of 3 in the computer time requirement originates from looking up 3 rather than 1 table for the potential.

In Fig. 3b also the dependence of the time factor α on the number of atoms N_c within the cut-off radius is shown. We used $N_c = 12, 18, 42$; these numbers correspond to a cut-off radius r_c in the middle between successive neighbor shells of the fcc crystal. Note the slow, sublinear increase of the cpu time with N_c, which is due to the heavy overhead which the molecular-dynamics program has to perform in addition to the force calculations.

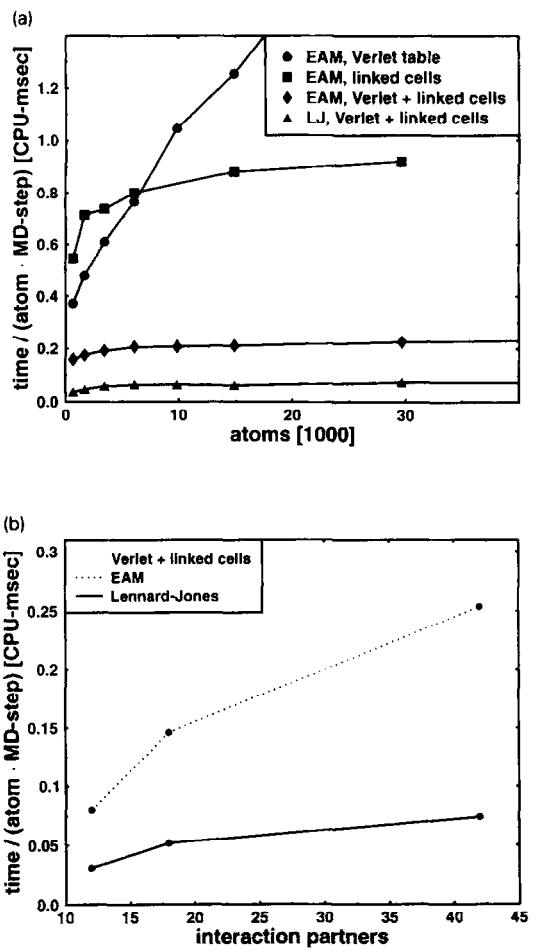

Fig. 3. Cpu time requirements per time step of the molecular-dynamics simulation and per atom. In all cases shown, the lists are updated every 5 time steps. (a) Influence of the neighbor list used, $N_c = 48$. For the fastest list structure, Verlet–linked-cells, a comparison between the requirements of a Lennard–Jones pair potential (LJ) and a many-body potential (EAM) is shown. (b) For a 3×10^4 atom system, and a Verlet–linked-cells neighbor list, the influence of the number of interaction partners, N_c, is shown.

It may be noted that force evaluation for covalent materials takes a longer time, since the structure of the forces is more complicated, and for 3-body forces the neighbor-list structure requires more thought, as neighbors of neighbors contribute to the force evaluation. Using the same computation parameters as in Fig. 3b (Verlet–linked-cells scheme, $N = 10^4$ particles), we find for the Stillinger–Weber potential [40], which uses a cut-off after the first neighbor shell ($N_c = 4$), a cost of 0.188 ms/atom/time-step, i.e., a considerable slow down with respect to metallic potentials.

Furthermore, we mention that the actual value of α given here depends on the programming language used. It is common folklore that FORTRAN is still the fastest language [81], even though the actual speed depends on the compiler and on the optimization options used. We checked our FORTRAN code against a C-program. The latter was around 20% slower.

Finally we wish to mention that the numbers given here depend on the actual machine used and on the skills of the programmer. In both respects our results may not be optimal.

Sometimes special measures are taken to speed up the code by using so-called moving-atom lists [66], such that forces are only calculated for atoms which have moved from their equilibrium position. Such a speed-up is particularly effective early after ion bombardment. It appears that such a measure is now rarely used due to the checks which need to be performed to ensure the unbiased functioning of the code. Ref. [82] reports on another optimization scheme for molecular-dynamics simulations, in which the distance which an atom moved, its acceleration, and other features are used to decide whether the force on the atom shall be calculated anew.

2.10. Reliability

Every numerical algorithm makes errors, viz. truncation and rounding errors. Furthermore, a sputtering simulation starts from a very strong non-equilibrium situation: one atom has all the energy, all the many others have none. A sufficiently long time after ion impact, the system will have thermalized. For such a scenario, it is well known that upon inversion of the particle momenta at such a late time, the initial non-equilibrium situation will never be re-established, since entropy has been created. In fact, the system is chaotic [11,78]: imagine a projectile which impinges directly on the center of a surface target atom; if the projectile is slightly displaced laterally, the insueing trajectory will look drastically different. This strong dependence on the initial condition is the signature of chaos; cf. also Fig. 2. As a result of the numerical errors and the chaos involved in our problem, individual ion trajectories and target atom cascades in the solid will look different from code to code, and from machine to machine, or even from simulation to simulation, if the "technical" parameters of the simulation, such as the time step, have been differently assigned, even if the same initial positions for the projectile and the target atoms have been chosen.

How then can one trust molecular-dynamics simulation results? From the above it appears that individual trajectories should be useful and reliable for short times, for example for the assessment of specific collision or emission mechanisms. The reliability of several molecular-dynamics codes for such short time scales has indeed been tested in round-robin computer simulations [83,84]; here fair agreement between these codes (and between them and BCA and MC simulations) could be established. In general, however, it is average values of the simulations which need to be compared between different codes, and only such averages can be compared to experiment. The requirement that a molecular-dynamics code gives a reliable estimate of the average quantities, such as the sputter yield, is equivalent with allowing a small numerical noise in the result of individual trajectories, under the condition that this noise is truly unbiased. Otherwise, the code introduces systematic errors.

The check of simulations by comparison to experiment is not always easily done. Many sputter experiments imply high ion fluences, under which the surface topography changes in an often not well characterized way. High-fluence simulations on the other hand are virtually impossible to perform, since these last a time which is too long compared to the ps- or ns-regime which can be simulated with the available computer power, and the influence of surface diffusion on surface topography is not easily assessed. Nowadays, however, more and more small-fluence experiments are under way, which lend themselves ideally to comparison with molecular-dynamics results, cf. Section 3.1.

Actually, two philosophies seem to exist: According to one of them, since the model itself is not perfect – the potential may be wrong, the target particle number is too small, etc. – why bother and calculate numbers with more than 10% accuracy, say? The other philosophy insists that molecular dynamics is in principle capable of predicting the outcome of a model sputter "experiment", in which only the interatomic potential enters as physical input; so it is worthwhile to calculate atom trajectories, sputter yields, etc., with high accuracy in order to check the model assumptions. According to the general ambition of reducing macroscopic phenomena to their atomistic causes, which stands behind the molecular-dynamics scheme, it is the author's opinion that the latter philosophy will survive.

3. Results

Molecular dynamics has been increasingly used in the last years as a theoretical tool for understanding sputtering. In this sense, this method competes with analytical theory, MC and BCA simulations. These latter methods have been primarily designed to describe the linear-cascade regime – although of course extensions are possible and have been experimented with [85], and in a sense, BCA simulations may be regarded as an approximation to molecular dynam-

ics. It might appear worthless if molecular-dynamics simulations were performed in the linear-cascade regime itself, since this method is considerably slower than the other three mentioned. However, as pointed out above, molecular dynamics appears to be the most realistic description of the sputter process. All effects possibly important for sputtering are included under the condition that a sufficiently reliable interatomic potential is supplied, and that the coupling to the electron system is realistically modeled. Hence, molecular-dynamics simulations in the linear-cascade regime aim at an accurate comparison to experimental data, or to a check of available analytical models, or are performed in order to provide parameters immediately from the potential for use in MC or BCA calculations or in analytical theory.

The range of applicability of molecular dynamics is limited to low bombarding energies by the number of atoms to be simulated. So the largest sputter simulation performed up to date is for a 20 keV Au atom bombarding a Au target [86]. Also in other ion–solid interaction simulations, only slightly higher energies have been employed, e.g. Ref. [87].

The true and original capability of molecular dynamics lies outside the regime of the linear cascade, viz. in the spike regime, and in the study of such phenomena as are induced by interatomic binding, such as cluster emission or chemical effects in sputtering. In these regimes, other theoretical or computational methods have difficulties.

It should be added that almost no molecular-dynamics simulations have been performed on laser sputtering, with the exception of strongly idealized model calculations [88]. The reason hereto is that – due to restrictions in simulation time – only ps- or sub-ps-laser-irradiation can be modelled; what is more important, the laser intensity is absorbed at least up to depths of 10 nm [89], even for UV lasers and strongly absorbing targets. As a consequence, not only the lateral, but also the depth scale of the relevant processes is quite large. In a recent presentation, both depth and lateral scale were strongly reduced, by increasing artificially the target absorptivity and by narrowing the laser beam to a nm-sized diameter [90]; as a result, the effects after laser irradiation looked very similar to cluster bombardment.

3.1. Linear-cascade regime

A number of molecular-dynamics studies have been performed in order to investigate basic issues in linear sputtering theory. The grouping of the results reported below under this heading may not appear fair in all cases. However, this section is meant to contain all those results that can be understood at least in a first approximation from the assumptions underlying linear-cascade theory, and refer to processes where neither atomic binding nor high energy densities play a strong role.

Progress has been reached in the field of preferential sputtering of alloys and compounds, a subject which is of considerable interest both in sputter applications and from a fundamental point of view [91]. In order to exploit the model

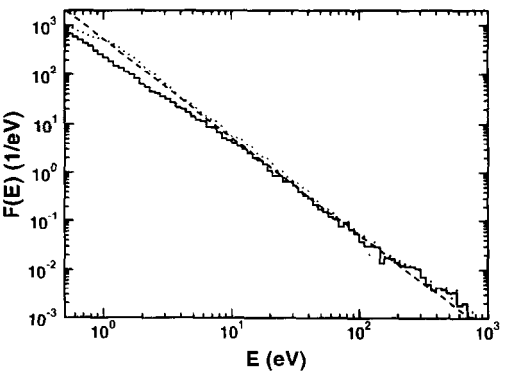

Fig. 4. Recoil density $F(E)$ calculated for 1 keV Cu bombardment of a Cu (100) surface, averaged over 100 ion impacts. The results of two molecular-dynamics simulations are shown. Dotted: purely repulsive interatomic interaction. Full: attraction included via a Morse potential. Dashed: prediction of linear-cascade theory, $\propto 1/E^2$. From Ref. [96].

character of molecular-dynamics calculations, it is useful to extend the simulations from realistic systems, such as the preferential sputtering of a CuNi alloy [92], to pseudo-alloys not found in nature. Thus, the sputtering of alloys with modified cohesive energies or heat of mixing could be studied and compared with the predictions of analytical theory; moreover, isotopic mixtures with unnaturally high mass ratio were studied, in order to enhance the effects found [93]. This latter trick has already been introduced earlier in preferential sputter simulations [94]. Further results on the subject of preferential sputtering have been obtained recently using BCA simulation methods [95].

A further problem which has been attacked is the influence of the so-called bulk-binding energy on collision cascade evolution. In Fig. 4, the recoil density $F(E)$ – i.e., the number of recoils generated in an energy window around E – is shown; this quantity was measured in the simulation by identifying E with the maximum kinetic energy reached by the recoil. Two different molecular-dynamics simulations are compared: one with a purely repulsive interaction potential, and another, where attractive forces are included. The figure shows that the recoil densities calculated in these two simulations are astonishingly similar and follow well the asymptotic $1/E^2$-behaviour predicted by linear-cascade theory. Only at small recoil energies, the influence of the attractive force becomes apparent. In Ref. [96], this influence has been related to the concept of the bulk-binding energy, which is used in analytical theory and MC or BCA calculations to incorporate the influence of interatomic attraction.

Another thread of work attempts to identify the role of electronic inelastic loss processes in a cascade, and of electron excitation [97,50,98]. As mentioned above in Section 2, such a procedure requires an ad hoc introduction of electronic processes into the simulation. The results achieved were also used to assess the mechanisms by which core-excited atoms are sputtered [99].

Also the work on understanding the sputter mechanisms of single crystals was continued. The evolution of this field

until 1992 is described in Ref. [100]. A special impetus for performing these simulations is provided by experimental techniques which allow to measure energy-resolved angular distributions of sputtered particles for small irradiation fluences and hence under well defined surface conditions. Such an experimental situation lends itself in an ideal way to molecular-dynamics simulations. In fact, it may be hoped that here it is only the interatomic interaction potential the knowledge of which limits the accuracy of the simulation; assuming that the other factors mentioned in Section 2 have been well taken care of. In this situation, a new potential – due to DePristo et al. [39,101] – was incorporated into the simulation, which was believed to describe interatomic interaction in metals in a more accurate way, and the sputter calculations which were previously performed with the EAM potential [102] were repeated. The new results appear to show a better agreement with experimental data [103].

Among further work on single-crystal sputtering we wish to mention Ref. [104], which aimed at identifying the mechanism of Wehner spot formation for low-energy sputtering, cf. also Ref. [105], and Ref. [106], where the temperature dependence of Wehner spots was investigated. Sputtering induced by hyperthermal rare-gas atoms bombarding different low-indexed surfaces of a Cu crystal was investigated in Ref. [107]. Other work tried to identify the differences between the sputtering of an amorphous in contrast to a single-crystal Si surface [108]; there also several discrepancies with previous simulation results of crystalline Si sputtering [66,109] are discussed.

Finally, some unusual work on linear-cascade sputtering should be mentioned. In condensed gases, very low-energy atoms – in the eV region – may give rise to so-called minicascades [56]. Such low energy atoms may be excited for instance by electronic excitation, and subsequent energy transfer to atomic motion. Molecular-dynamics simulations of this phenomenon have been performed with the aim of describing electronic sputtering in condensed gases [110] and the transmission of atoms through thin rare-gas films, and the concomitant sputtering [111].

3.2. High-energy density (spike) phenomena

The linear-cascade sputter regime is left as soon as the energy imparted per atom E_{atom} in a certain subvolume of the cascade becomes at least of the order of the cohesive energy E_{coh} of the solid. If this happens close enough to the surface, dramatic sputter phenomena may happen. In fact, since sputtering is a stochastic phenomenon, in a particular system some ion trajectories may lead to spike formation, while others may not. The idea that regions of high energy density may lead to prolific sputtering is rather old, see quotations in Ref. [112]. Molecular-dynamics simulations could show its existence and relevance first in the case of sputtering of condensed noble gases, where the cohesive energy is so small that the above mentioned criterion is readily reached [113,114]. More recently, the transition from linear to nonlinear sputtering was investigated in such systems [115]. Sputtering of a condensed molecular gas (N_2) was studied in Ref. [116].

Spike phenomena were also found for polyethylene bombardment [117], and in the case of metals. In the latter case, for 20 keV Au bombardment of a Au target, a trajectory was shown which led to dramatic atom emission [86]. Of course, this was a single trajectory and the statistical significance of this event is small; at higher bombarding energies, around the maximum of the nuclear stopping power, a substantial, if not dominant, contribution from spikes is measured experimentally for Au [118,119].

We exemplify a spike in Fig. 1 for the case of 5 keV Cu → Cu bombardment. The color code denotes the "temperature" of the atoms in the following sense: around each atom, the average of the kinetic energy of all atoms within a sphere of radius r_c (the interaction cut-off radius) in the center-of-mass system is taken, and converted to units of temperature. Thus, the "temperature" of all sputtered monatomics is zero, while that of the small clusters is equivalent to their internal energy. Within the solid, the "temperature" 1 ps after bombardment is at some places considerably above the melting temperature of Cu of 1358 K.

Another way to produce high energy densities inside the bombarded material is by cluster bombardment. In fact, in the recent past, the consequences of bombarding surfaces with clusters have been investigated by molecular dynamics for the purpose of identifying the basic interaction mechanisms of clusters with solids [120–127], and to model cluster deposition [64,128–130], but only to a small extent for the immediate purpose of sputtering [121,131]; see Ref. [119] for a recent review. There can be no doubt, however, that the high energy densities, which are usually delivered by clusters will give rise to interesting spike phenomena. The related issue of fullerene bombardment and the induced sputtering has been more thoroughly attacked by molecular dynamics [132].

High energy densities may also be reached in ion tracks. These are produced by swift ions, typically fission fragments, which penetrate on a straight line through the material and deliver energy mainly in the form of electronic excitation, which is subsequently converted into nuclear motion. The sputtering from high-energy-density tracks has been investigated by molecular-dynamics simulations as a function of E_{atom}/E_{coh} [133].

Spikes may be rather long lived – on the order of 1 to several ps –, whereas linear collision cascades have died after several 100 fs after ion impact, when the energy of all atoms has decreased below the cohesive energy, and hence no more collision-cascade sputtering can occur. The reason hereto is that in a spike, energy has more or less been equilibrated between all the atoms, and hence its lifetime is governed by energy diffusion (heat conduction) out of the spike volume, while in a linear collision cascade each moving atom loses energy when it collides with an atom at rest. Hence it is a question of main importance to the lifetime of

spikes whether electrons can participate in energy dissipation. Various schemes have been proposed to include electrons into a molecular-dynamics simulation in a phenomenological way [14,51–55]. One result of these considerations is that for good electrical conductors – such as Cu or Ag – the coupling between electrons and atoms is too small to sensibly affect the lifetime of a spike; in other cases – such as Ni or Pt –, however, spikes may be efficiently quenched by electronic heat conduction [53,54]. Even arguments were raised that in some cases energy may be imparted from the electrons to the phonon systems. Such a situation may be important for high-energy irradiation (in the MeV region) where a nonnegligible part of the projectile energy is given to the electronic system, and may be imparted from the electrons to the atoms [134].

3.3. Cluster emission

For most classes of materials, interatomic bonding is affected by the environment. Thus, for instance in Cu, the dimer binding energy in vacuum is 2 eV; the binding energy between 2 atoms in solid Cu – which might in zeroth approximation be defined by dividing the cohesive energy E_{coh} = 3.5 eV by half the number of nearest neighbors, 6 – is only around 0.6 eV. Note that during the cluster formation process, the bonding of an atom changes from the solid or surface environment continuously to a cluster environment in which the atom is usually much lower coordinated. Molecular-dynamics simulations appear ideally suited to realistically describe this process. It is hard to imagine how other simulational tools could achieve this crucial task without the introduction of ad hoc assumptions.

This shows that in many materials, such as in metals or in covalent materials, a realistic description of cluster formation and emission in sputtering depends on the availability of a potential which describes as well the binding of clusters and in the solid. The many-body potentials used in sputter simulations are able to describe these changes in binding at least in a qualitative way [31]. In the case of metals, there is a potential available which has been specifically designed to describe the binding in both dimers and solids quite accurately [39,101].

The most abundant form of clusters sputtered are dimers. In many experiments performed by keV bombardment of metals, a fraction of some 10% of the sputtered atoms are bound as dimers; therefore quite a large body of information on sputtered dimers has been assembled in the past, and has been reviewed in Ref. [72]. New information has been obtained recently [105,135–137]. As an example, it might be mentioned that by the judicious construction of metallic materials, where the cohesive energy and the heat of mixing can be more or less arbitrarily assigned to the pseudo-alloy formed, it was possible to show in which manner the dimer yield decreases with increasing surface-binding energy of the atoms, and increases with increasing dissociation energy of the dimer [137].

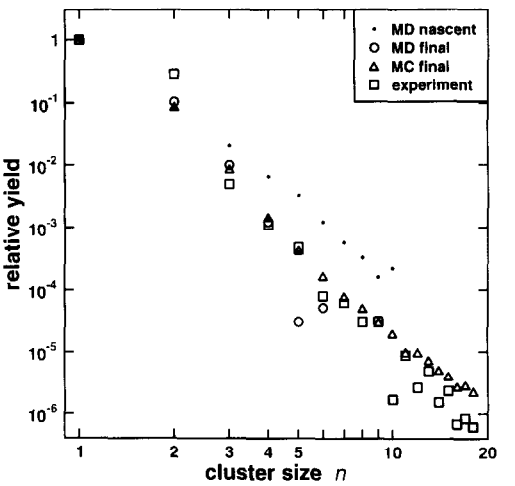

Fig. 5. Relative abundance distribution $Y(n)$ of Ag_n clusters sputtered from a Ag (111) surface due to 5 keV Ar bombardment. Nascent and final distributions calculated by molecular dynamics immediately after, and 500 ps after ion emission. Monte Carlo results, extrapolated from molecular-dynamics data as described in the text. Experimental data from Ref. [157]. Plotted after Ref. [59] with permission of the author.

Another feature which has already been studied in some detail by molecular dynamics in the past was molecule sputtering; i.e., the emission of preformed molecules from the surface. Sputtering of adsorbed molecules and their fragmentation were investigated in Refs. [138,139]; cf. also the work on polyethylene mentioned above [117].

A particularly fascinating feature of the sputter phenomenon is that quite large clusters may be emitted. For example, in an experiment on keV bombardment of Ag, Ag clusters up to Ag_{18} have been found [140]; the upper limit is restricted only by the resolution of the experimental detector, rather than by the size of the clusters actually emitted. Similar results have been observed by other groups [141]. It is highly interesting to gain information on the properties of these clusters and in particular on the mechanisms how they are formed. In principle, molecular-dynamics simulations are able to deliver this information; however, since large-cluster emission is a rare event, a huge number of atom impacts has to be simulated in order to gain statistically relevant information. New results have been produced in particular in Refs. [59,60]. Fig. 5 shows such a piece of information gained. Here, a high-sputter-yield system was chosen – 5 keV Ar → Ag(111)– and modeled with a potential [39,101], which reproduces satisfactorily the cluster binding properties.

As a result, clusters up to a size n = 10 were observed to be sputtered in the molecular-dynamics simulation. However, many of these contained such a high amount of internal energy that they decayed very quickly, on a time scale of 1 ps to several 100 ps, depending on the internal excitation; clusters with an internal excitation just above the dissociation threshold can even live much longer, and can be detected experimentally as metastable clusters on a μs time scale [72].

By calculating the fragmentation process with molecular dynamics, the distribution of stable clusters could be determined. These results were then extrapolated towards larger clusters by a special MC routine built as a post-processor of the molecular-dynamics data; the MC routine incorporates cluster fragmentation via the RRK transition-state theory of unimolecular decay. The result of this simulation shows an astonishingly good overall agreement with the measured data. The cluster abundance distribution follows a power-law decay; a transparent argument for its origin is still missing.

3.4. Surface topography formation

As evidenced in Fig. 1, ion bombardment leads not only to particle emission from the surface but also to the formation of surface topography. In the violent case depicted in Fig. 1, it is evidently a near-surface spike which is the cause of the large bulge of atoms which extrudes from the surface. In the linear-cascade regime, the main topographical feature will be the formation of adatoms on the surface; adatoms may be considered to be those atoms which have been kicked out of the surface by the collision cascade, but whose momentum was not sufficient to pass the surface barrier. While the formation of large hillocks or craters on the surface has been demonstrated by molecular dynamics in several instances (cf. also Fig. 1), no systematic investigation of this phenomenon seems to have been performed. Adatom formation, on the other hand, has been investigated more systematically. In an investigation of the sputtering of Pt(111) by keV noble gas ions, it was found that the number of adatoms formed was roughly a factor of 4 times higher than the sputter yield [142]; this is in agreement with experiment [143].

Of course, surface topographical structures may strongly change with time after bombardment. Surface diffusion, which is strongly temperature dependent, will be a main reason for surface changes, but not the only one. While this issue is relevant for many applications, and has been studied theoretically quite extensively [144,145], it seems hard to perform dedicated molecular-dynamics studies of this process.

3.5. Effects of surface topography

The formation of surface topographical structures may affect the sputtering behavior of the surface. In craters, for instance, redeposition will act to lower the sputter yield. Due to the general dependence of the sputter yield on the incidence angle of the bombarding ion, any large-scale (i.e., on the length of a cascade dimension) surface structure will change the incidence angle of the bombarding ion with respect to the local surface normal. Calculations of such a phenomenon have been performed [146,147], but not on a molecular-dynamics basis.

However, some molecular-dynamics information exists on the influence of a microscopically rough surface on the sputter yield [67]. To this end, a Pt(111) surface was randomly

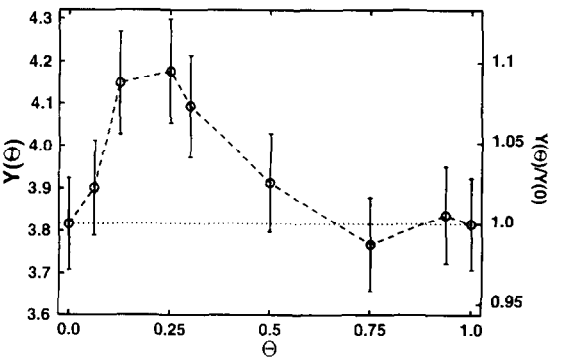

Fig. 6. Dependence of the sputter yield Y of a 1 keV Ar bombarded Pt(111) surface on the adatom coverage Θ. Dashed lines are to guide the eye. Dotted: yield of an adatom-free surface, $Y(0)$. From Ref. [67].

covered with a definite coverage Θ. The change of the sputter yield of this surface with coverage is shown in Fig. 6 for 1 keV Ar bombardment. It is seen that the effect is small, of the order of 10%. This is reassuring in view of the fact that sputter theory employs a mean, site-independent value for the surface binding. Interestingly, the yield enhancement is most pronounced for small coverages, $\Theta < 0.5$, while for a more than half-filled layer of atoms, almost no change of the sputter yield with respect to a clean surface is found. This asymmetry is due to two effects: (i) Sputtering is easiest for isolated adatoms, which are the weakest bound to the surface; these are most frequently found for small coverage. (ii) For large coverage, the energetic benefit of sputtering atoms from the adatom layer is balanced by the geometric restriction of sputtering atoms from the original surface layer due to blocking by the adatoms. It should be mentioned that due to the metallic binding assumed in this calculation, the effect is smaller than for a pair interaction potential. Taking this into account, the results shown here are in agreement with earlier simulations which were performed for half a monolayer coverage, $\Theta = 0.5$, and for pair potential interaction [148].

The effect of surface topography may be considerably stronger in the case of covalent materials with their directional bonding, as has been discussed in Section 2.4. A detailed study of the effect of 225 eV Xe bombardment on the surface topography evolution of Si(111) and the influence of this topography on the sputtering mechanism has been published recently [149]; the resulting layer-by-layer sputter mode is consistent with experiment [150].

3.6. Chemical effects

Chemistry may play different roles in sputter problems. They range from atom-specific surface-binding energies in alloys or compounds, over bond breaking or re-organization in compounds or molecular targets upon ion irradiation, to ion-beam etching, where the addition of a reaction partner of the target material during sputtering increases the sputter yield in a synergistic way. Several aspects of chemical pro-

cesses have been already addressed above under the heading of dimer emission, and the polyethylene bombardment study mentioned under spike phenomena.

After the availability of potentials for thermal surface reactions – such as the thermal etching of a Si surface by F atoms – was demonstrated [151], dedicated studies of reactive ion-etching phenomena have been performed more recently [152,153]. The system studied was 200 eV Ar bombardment of Si in a Cl atmosphere. The simulations were used to interpret the synergetics of chemical sputtering, and the emission mechanisms of low-energy reaction products. In other work, the sputtering of a H-terminated Si-surface by low-energy ion irradiation was studied [154].

Chemical effects can only be modelled if potentials are available which include the chemistry at least in a qualitative way [155]. A prominent example of such a potential is the so-called Brenner potential [156], an example of the class of bond-order potentials [42]. It has been found to describe well the chemistry of hydrocarbons.

4. Conclusions

Molecular-dynamics simulations are increasingly used in order to gain a microscopic understanding of the atomistic mechanisms underlying ion–solid interaction phenomena in general, and sputtering in particular. Their physical input is mainly the interatomic potential used; however, effects of electronic excitation, the initial state of the target, and the influence of boundary conditions, which must be used to model the influence of the surrounding material, may also affect the results. Besides these more physical issues, the reliability of computer simulation results depends on a number of technical questions: the choice of the time step for the integrator used, the simulation termination criterion, details of the sputtered-particle detector (in particular for clusters), and the care with which sufficient statistics has been gathered.

While the field of linear-cascade sputtering appears to be sufficiently well understood by means of analytical theory, BCA and MC simulations, also molecular-dynamics simulations have been performed for such systems; the advantage is here that in principle – i.e., with the restrictions mentioned above – all sputter characteristics can be traced back to the interatomic potential; all the other parameters used elsewhere – such as the surface- and bulk-binding energy – need not to be introduced in a molecular-dynamics simulation. In this sense molecular dynamics gives a very holistic view of sputtering, and it is indeed attempted to gain an accurate description of selected low-fluence experiments on well-characterized surfaces by molecular-dynamics simulations.

More original and creative applications of molecular dynamics are found in sputter processes outside the linear-cascade regime. Examples given include sputtering from spikes (high-energy density zones), the influence of attractive forces during sputtering, such as in cluster emission, the formation and influence of surface topography, and effects of chemistry.

Acknowledgements

Thanks are due to G. Betz, R. Smith, M. Vicanek, T.J. Colla, P. Klein, and H. Hensel for critical comments on the manuscript. T.J. Colla is specially acknowledged for performing the calculations leading to Figs. 1–3, and A. Wucher for giving me his data to prepare Fig. 5.

References

[1] R. Behrisch (ed.), Sputtering by particle bombardment I (Springer, Berlin, 1981).
[2] R. Behrisch (ed.), Sputtering by particle bombardment II (Springer, Berlin, 1983).
[3] R. Behrisch and K. Wittmaack (eds.), Sputtering by particle bombardment III (Springer, Berlin, 1991).
[4] P. Sigmund (ed.), Fundamental Processes in Sputtering of Atoms and Molecules (SPUT92), K. Dan. Vidensk. Selsk. Mat. Fys. Medd. 43 (1993) entire volume.
[5] R. Kelly and A. Miotello, in: Pulsed Laser Deposition of Thin Films, eds. D.B. Chrisey and G.K. Hubler (Wiley, New York, 1994) p. 55.
[6] J.B. Gibson, A.N. Goland, M. Milgram and G.H. Vineyard, Phys. Rev. 120 (1960) 1229.
[7] P. Sigmund, Phys. Rev. 184 (1969) 383.
[8] M.T. Robinson and I.M. Torrens, Phys. Rev. 9 (1974) 5008.
[9] J.P. Biersack and W. Eckstein, Appl. Phys. A 34 (1984) 73.
[10] W. Eckstein, Computer Simulation of Ion–Solid Interactions (Springer, Berlin, 1991).
[11] H.H. Andersen, Nucl. Instr. and Meth. B 18 (1987) 321.
[12] D.E. Harrison, Jr., Crit. Rev. Solid State Mater. Sci. 14 (1988) S1.
[13] M.T. Robinson, K. Dan. Vidensk. Selsk. Mat. Fys. Medd. 43 (1993) 27.
[14] R.M. Nieminen, K. Dan. Vidensk. Selsk. Mat. Fys. Medd. 43 (1993) 81.
[15] G. Galli and A. Pasquarello, in: Computer Simulation in Chemical Physics, eds. M.P. Allen and D.J. Tildesley (Kluwer, Dordrecht, 1993) NATO ASI E: Applied Sciences, Vol. 397, p. 261.
[16] S. Uhlmann, T. Frauenheim and U. Stephan, Phys. Rev. B 51 (1995) 4541.
[17] H. Hensel, P. Klein, H.M. Urbassek and T. Frauenheim, Phys. Rev. B 53 (1996) 16497.
[18] J.R. Beeler, Jr., Radiation Effects Computer Experiments (North-Holland, Amsterdam, 1983).
[19] Molecular-dynamics simulation of statistical-mechanical systems, eds. G. Ciccotti and W.G. Hoover (North-Holland, Amsterdam, 1986).
[20] M.P. Allen and D.J. Tildesley (eds.), Computer Simulation of Liquids (Clarendon, Oxford, 1987).
[21] V. Vitek and D.J. Srolovitz (eds.), Atomistic Simulation of Materials: Beyond Pair Potentials (Plenum, New York, 1989).
[22] C.R.A. Catlow, S.C. Parker and M.P. Allen (eds.), Computer Modelling of Fluids, Polymers and Solids, NATO ASI E: Applied Sciences, Vol. 293 (Kluwer, Dordrecht, 1990).
[23] M. Meyer and V. Pontikis (eds.), Computer Simulation in Materials Science, NATO ASI E: Applied Sciences, Vol. 205 (Kluwer, Dordrecht, 1991).
[24] J.M. Haile, Molecular Dynamics Simulation (Wiley, New York, 1992).
[25] M.P. Allen and D.J. Tildesley (eds.), Computer Simulation in Chemical Physics, NATO ASI E: Applied Sciences, Vol. 397 (Kluwer, Dordrecht, 1993).

[26] C.A. English, J.R. Matthews, H. Rauh, A.M. Stoneham and R. Thetford (eds.), Materials Modelling: From Theory to Technology (IOP, Bristol, 1992).
[27] A.F. Voter, MRS Bull. 21(2) (1996) 17.
[28] G. Molière, Z. Naturforsch. A 2 (1947) 133.
[29] W.D. Wilson, L.G. Haggmark and J.P. Biersack, Phys. Rev. B 15 (1977) 2458.
[30] J.F. Ziegler, J.P. Biersack and U. Littmark, Stopping Powers and Ranges of Ions in Matter, Vol. 1 (Pergamon, New York, 1985).
[31] A.E. Carlsson, in: Solid State Physics, Vol. 43, eds. H. Ehrenreich and D. Turnbull (Academic Press, Boston, 1990) p. 1.
[32] M.S. Daw and M.I. Baskes, Phys. Rev. B 29 (1984) 6443.
[33] M.S. Daw, S.M. Foiles and M. Baskes, Mat. Sci. Rep. 9 (1993) 251.
[34] S.M. Foiles, MRS Bull. 21(2) (1996) 24.
[35] F. Ducastelle, J. Phys. (Paris) 31 (1970) 1055.
[36] M.W. Finnis and J.E. Sinclair, Philos. Mag. A 50 (1984) 45; 53 (1986) 161.
[37] F. Ducastelle, in: Computer Simulation in Materials Science, eds. M. Meyer and V. Pontikis, NATO ASI E: Applied Sciences, vol. 205 (Kluwer, Dordrecht, 1991) p. 223.
[38] K.W. Jacobsen, J.K. Nørskov and M.J. Puska, Phys. Rev. B 35 (1987) 7423.
[39] T.J. Raeker and A.E. DePristo, Int. Rev. Phys. Chem. 10 (1991) 1.
[40] F.H. Stillinger and T.A. Weber, Phys. Rev. B 31 (1985) 5262.
[41] J. Tersoff, Phys. Rev. Lett. 56 (1986) 632.
[42] D.W. Brenner, MRS Bull. 21(2) (1996) 36.
[43] J.J. Salacuse and P.A. Egelstaff, Phys. Rev. A 38 (1988) 4313.
[44] P. Vashishta, R.K. Kalia, J.R. Rino and I. Ebbsjö, Phys. Rev. B 41 (1990) 12197.
[45] A. Nakano, R.K. Kalia and P. Vashishta, Phys. Rev. Lett. 73 (1994) 2336.
[46] M. Jentschel, K.H. Heinig, H.G. Börner, J. Jolie and E.G. Kessler, Nucl. Instr. and Meth. B 115 (1996) 446.
[47] H.H. Andersen, Appl. Phys. 18 (1979) 131.
[48] W. Schilling and H. Ullmaier, in: Nuclear Materials, Part 2, eds. R.W. Cahn, P. Haasen and R.J. Kramer (VCH, Weinheim, 1994) Materials Science and Technology, Vol. 10B, p. 179.
[49] D.E. Harrison, Jr. and M.M. Jakas, Nucl. Instr. and Meth. B 15 (1986) 25.
[50] M.H. Shapiro and T.A. Tombrello, Nucl. Instr. and Meth. B 94 (1994) 186.
[51] C.P. Flynn and R.S. Averback, Phys. Rev. B 38 (1988) 7118.
[52] A. Caro and M. Victoria, Phys. Rev. A 40 (1989) 2287.
[53] M.W. Finnis, P. Agnew and A.J.E. Foreman, Phys. Rev. B 44 (1991) 567.
[54] I. Koponen, J. Appl. Phys. 72 (1992) 1194.
[55] A. Caro, Radiat. Eff. Defects Solids 130 & 131 (1994) 187.
[56] R.E. Johnson and J. Schou, K. Dan. Vidensk. Selsk. Mat. Fys. Medd. 43 (1993) 403.
[57] S.T. Cui, R.E. Johnson, C.T. Reimann and J.W. Boring, Phys. Rev. B 39 (1989) 12345.
[58] M. Hou and Z.-Y. Pan, Nucl. Instr. and Meth. B 102 (1995) 93.
[59] A. Wucher and B.J. Garrison, J. Chem. Phys. (1996) in press.
[60] G. Betz and W. Husinsky, Nucl. Instr. and Meth. B 102 (1995) 281.
[61] Y. Wu and R.J. Friauf, J. Appl. Phys. 65 (1989) 4714.
[62] C.M. Gilmore and J.A. Sprague, Phys. Rev. B 44 (1991) 8950.
[63] J.C. Tully, J. Chem. Phys. 73 (1980) 1975.
[64] H. Haberland, Z. Insepov and M. Moseler, Phys. Rev. B 51 (1995) 11061.
[65] J. Laakkonen and R.M. Nieminen, Phys. Rev. B 41 (1990) 3978.
[66] R. Smith, D.E. Harrison, Jr. and B.J. Garrison, Phys. Rev. B 40 (1989) 93.
[67] T.J. Colla and H.M. Urbassek, Nucl. Instr. and Meth. B 117 (1996) 361.
[68] C.W. Gear, Numerical Initial Value Problems in Ordinary Differential Equations (Prentice-Hall, Englewood Cliffs, 1971).
[69] D.W. Brenner and B.J. Garrison, Phys. Rev. B 34 (1986) 5782.
[70] R. Smith and D.E. Harrison, Jr., Comput. Phys. 3 (5) (1989) 68.
[71] R. Smith, private communication.
[72] H.M. Urbassek and W.O. Hofer, K. Dan. Vidensk. Selsk. Mat. Fys. Medd. 43 (1993) 97.
[73] U. Conrad and H.M. Urbassek, Nucl. Instr. and Meth. B 48 (1990) 399.
[74] J.M. Hammersley and D.C. Handscomb, Monte Carlo Methods (Chapman and Hall, London, 1979).
[75] F. James, Rep. Prog. Phys. 43 (1980) 1145.
[76] W.H. Press and S.A. Teukolsky, Comput. Phys. 3(6) (1989) 77.
[77] W.H. Press, B.P. Flannery, S.A. Teukolsky and W.T. Vetterling, Numerical Recipes (Cambridge University Press, Cambridge, 1989).
[78] M.T. Robinson, Nucl. Instr. and Meth. B 90 (1994) 509.
[79] G.S. Grest, B. Dünweg and K. Kremer, Comput. Phys. Commun. 55 (1989) 269.
[80] L. Verlet, Phys. Rev. 159 (1967) 98.
[81] S.W. Haney, Comput. Phys. 8 (1994) 690.
[82] H. Zhu and R.S. Averback, Nucl. Instr. and Meth. B 83 (1993) 334.
[83] P. Sigmund, M.T. Robinson, M.I. Baskes, M. Hautala, F.Z. Cui, W. Eckstein, Y. Yamamura, S. Hosaka, T. Ishitani, V.I. Shulga, D.E. Harrison, Jr., I.R. Chakarov, D.S. Karpuzov, E. Kawatoh, R. Shimizu, S. Valkealahti, R.M. Nieminen, G. Betz, W. Husinsky, M.H. Shapiro, M. Vicanek and H.M. Urbassek, Nucl. Instr. and Meth. B 36 (1989) 110.
[84] K. Gärtner, D. Stock, B. Weber, G. Betz, M. Hautala, G. Hobler, M. Hou, S. Sarite, W. Eckstein, J.J. Jimenez-Rodriguez, A.M.C. Perez-Martin, E.P. Andribet, V. Konoplev, A. Gras-Marti, M. Posselt, M.H. Shapiro, T.A. Tombrello, H.M. Urbassek, H. Hensel, Y. Yamamura and W. Takeuchi, Nucl. Instr. and Meth. B 102 (1995) 183.
[85] Y. Yamamura, Nucl. Instr. and Meth. B 33 (1988) 493.
[86] M. Ghaly and R.S. Averback, Phys. Rev. Lett. 72 (1994) 364.
[87] T. Diaz de la Rubia and M.W. Guinan, Phys. Rev. Lett. 66 (1991) 2766.
[88] T.J. Colla and H.M. Urbassek, Comput. Mater. Sci. 6 (1996) 7.
[89] S. Preuss, A. Demchuk and M. Stuke, Appl. Phys. A 61 (1995) 33.
[90] R.F.W. Herrmann, J. Gerlach and E.E.B. Campbell, Nucl. Instr. and Meth. B (1996) (accepted).
[91] P. Sigmund and N.Q. Lam, K. Dan. Vidensk. Selsk. Mat. Fys. Medd. 43 (1993) 255.
[92] N.Q. Lam and K. Johannessen, Nucl. Instr. and Meth. B 71 (1992) 371.
[93] H. Gades and H.M. Urbassek, Nucl. Instr. and Meth. B 102 (1995) 261.
[94] M.H. Shapiro, P.K. Haff, T.A. Tombrello and D.A. Harrison, Nucl. Instr. Meth. B 30 (1988) 152.
[95] V.I. Shulga and P. Sigmund, Nucl. Instr. and Meth. B 103 (1995) 383.
[96] H.M. Urbassek, G. Mayer, H. Gades and M. Vicanek, Nucl. Instr. and Meth. B 103 (1995) 275.
[97] M.H. Shapiro and T.A. Tombrello, Nucl. Instr. and Meth. B 90 (1994) 473.
[98] M.H. Shapiro and T.A. Tombrello, Nucl. Instr. and Meth. B 102 (1995) 277.
[99] M.H. Shapiro and T.A. Tombrello, Nucl. Instr. and Meth. B 66 (1992) 317.
[100] N. Winograd, K. Dan. Vidensk. Selsk. Mat. Fys. Medd. 43 (1993) 223.
[101] M.S. Stave, D.E. Sanders, T.J. Raeker and A.E. DePristo, J. Chem. Phys. 93 (1990) 4413.
[102] R. Maboudian, Z. Postawa, M. El-Maazawi, B.J. Garrison and N. Winograd, Phys. Rev. B 42 (1990) 7311.
[103] S.W. Rosencrance, J.S. Burnham, D.E. Sanders, C. He, B.J. Garrison, N. Winograd, Z. Postawa and A.E. DePristo, Phys. Rev. B 52 (1995) 6006.
[104] K. Johannessen, Nucl. Instr. and Meth. B 71 (1992) 171.
[105] G. Betz, R. Kirchner, W. Husinsky, F. Rüdenauer and H.M. Urbassek, Radiat. Eff. Defects Solids 130 & 131 (1994) 251.
[106] S.W. Rosencrance, N. Winograd, B.J. Garrison and Z. Postawa, Phys. Rev. B 53 (1996) 2378.
[107] H. Gades and H.M. Urbassek, Appl. Phys. A 61 (1995) 39.
[108] J.E. Rubio, L.A. Marques, M. Jaraiz, L.A. Bailon and J. Babolla, Nucl. Instr. and Meth. B 102 (1995) 301.
[109] R.A. Stansfield, K. Broomfield and D.C. Clary, Phys. Rev. B 39 (1989) 7680.
[110] R.E. Johnson and M. Liu, J. Chem. Phys. 104 (1996) 6041.
[111] P. Klein, H.M. Urbassek and M. Vicanek, Phys. Rev. B 51 (1995) 4597.
[112] P. Sigmund, in: Sputtering by Particle Bombardment I, eds. R. Behrisch (Springer, Berlin, 1981) p. 9.

[113] H.M. Urbassek and K.T. Waldeer, Phys. Rev. Lett. 67 (1991) 105.
[114] K.T. Waldeer and H.M. Urbassek, Nucl. Instr. and Meth. B 73 (1993) 14.
[115] L. Dutkiewicz, R. Pedrys, J. Schou and K. Kremer, Phys. Rev. Lett. 75 (1995) 1407.
[116] H. Kafemann and H.M. Urbassek, Mod. Phys. Lett. B 7 (1993) 857.
[117] K. Beardmore and R. Smith, Nucl. Instr. and Meth. B 102 (1995) 223.
[118] H.L. Bay, H.H. Andersen, W.O. Hofer and O. Nielsen, Nucl. Instr. and Meth. 132 (1976) 301.
[119] H.H. Andersen, K. Dan. Vidensk. Selsk. Mat. Fys. Medd. 43 (1993) 127.
[120] V.I. Shulga, M. Vicanek and P. Sigmund, Phys. Rev. A 39 (1989) 3360.
[121] V.I. Shulga and P. Sigmund, Nucl. Instr. and Meth. B 62 (1991) 23.
[122] R.S. Averback, T. Diaz de la Rubia, H. Hsieh and R. Benedek, Nucl. Instr. and Meth. B 59/60 (1991) 709.
[123] H. Hsieh, R.S. Averback, H. Sellers and C.P. Flynn, Phys. Rev. B 45 (1992) 4417.
[124] Z. Pan, Nucl. Instr. and Meth. B 66 (1992) 325.
[125] R.S. Averback and M. Ghaly, Nucl. Instr. and Meth. B 90 (1994) 191.
[126] R.S. Averback, M. Ghaly and H. Zhu, Radiat. Eff. Defects Solids 130 & 131 (1994) 211.
[127] Z.Y. Pan and M. Hou, Nucl. Instr. and Meth. B 102 (1995) 317.
[128] H. Hsieh and R.S. Averback, Phys. Rev. B 42 (1990) 5365.
[129] H. Hsieh and R.S. Averback, Nucl. Instr. and Meth. B 59/60 (1991) 203.
[130] H. Haberland, Z. Insepov and M. Moseler, Z. Phys. D 26 (1993) 229.
[131] K. Johannessen, Nucl. Instr. and Meth. B 73 (1993) 481.
[132] R. Smith, K. Beardmore, A. Gras-Marti, R. Kirchner and R.P. Webb, Nucl. Instr. and Meth. B 102 (1995) 211.
[133] H.M. Urbassek, H. Kafemann and R.E. Johnson, Phys. Rev. B 49 (1994) 786.
[134] I. Koponen and M. Hautala, Nucl. Instr. and Meth. B 93 (1994) 374.
[135] F. Karetta and H.M. Urbassek, Appl. Phys. A 55 (1992) 364.
[136] M.H. Shapiro and T.A. Tombrello, Nucl. Instr. and Meth. B 84 (1994) 453.
[137] H. Gades and H.M. Urbassek, Nucl. Instr. and Meth. B 103 (1995) 131.
[138] R.S. Taylor and B.J. Garrison, Chem. Phys. Lett. 230 (1994) 495.
[139] R.S. Taylor, C.L. Brummel, N. Winograd, B.J. Garrison and J.C. Vickerman, Chem. Phys. Lett. 233 (1995) 575.
[140] A. Wucher, M. Wahl and H. Oechsner, Nucl. Instr. and Meth. B 82 (1993) 337.
[141] S.R. Coon, W.F. Calaway, M.J. Pellin and J.M. White, Surf. Sci. 298 (1993) 161.
[142] H. Gades and H.M. Urbassek, Phys. Rev. B 50 (1994) 11167.
[143] T. Michely and C. Teichert, Phys. Rev. B 50 (1994) 11156.
[144] J. Rudnick and R. Bruinsma, in: Low Energy Ion-Surface Interactions, ed. J.W. Rabalais (Wiley, Chichester, 1994) p. 535.
[145] G. Carter, V. Vishnyakov and M.J. Nobes, Nucl. Instr. and Meth. B 115 (1996) 440.
[146] P. Sigmund, J. Mater. Sci. 8 (1973) 1545.
[147] U. Littmark and W.O. Hofer, J. Mater. Sci. 13 (1978) 2577.
[148] G. Betz, M.J. Pellin, J.W. Burnett and D.M. Gruen, Nucl. Instr. and Meth. B 58 (1991) 429.
[149] V.A. Zinovyev, L.N. Aleksandrov, A.V. Dvurechenskii, K.-H. Heinig and D. Stock, Thin Solid Films 241 (1994) 167.
[150] P. Bedrossian and T. Klitsner, Phys. Rev. B 44 (1991) 13783.
[151] P.C. Weakliem, C.J. Wu and W.A. Carter, Phys. Rev. Lett. 69 (1992) 200.
[152] H. Feil, J. Dieleman and B.J. Garrison, J. Appl. Phys. 74 (1993) 1303.
[153] H. Feil, Phys. Rev. Lett. 74 (1995) 1879.
[154] M.V.R. Murty and H.A. Atwater, Nucl. Instr. and Meth. B 102 (1995) 293.
[155] B.J. Garrison and D. Srivastava, Ann. Rev. Phys. Chem. 46 (1995) 373.
[156] D.W. Brenner, Phys. Rev. B 42 (1990) 9458.
[157] M. Wahl and A. Wucher, Nucl. Instr. and Meth. B 94 (1994) 36.